Elucidating Lewis acidity of metal sites in MFU-4l metal-organic frameworks: N$_2$O and CO$_2$ adsorption in MFU-4l, Cu^I-MFU-4l and Li-MFU-4l

Dmytro Denysenko [a], Jelena Jelic [b], Oxana V. Magdysyuk [c], Karsten Reuter [b], Dirk Volkmer [a], [*]

[a] Institute of Physics, Chair of Solid State and Materials Chemistry, University of Augsburg, Universitätsstrasse 1, D-86159 Augsburg, Germany
[b] Chair of Theoretical Chemistry and Catalysis Research Center, Technische Universität München, Lichtenbergstr. 4, D-85747 Garching, Germany
[c] Diamond Light Source Ltd., Harwell Science and Innovation Campus, OX11 0DE Didcot, United Kingdom

1. Introduction

Metal-organic frameworks (MOFs) represent an exponentially growing class of functional porous materials featuring well defined pore structures, high internal surface areas, high thermal and chemical stability as well as possibility to vary pore size and chemical or physical properties [1]. MOFs have been extensively studied as materials for the capture of gases and vapors [2,3] and for gas separation and storage [4–6]. Despite of the huge number of publications on gas sorption, adsorption of nitrous oxide (N$_2$O) has only rarely been studied. Thus, to the best of our knowledge, it was only once described for MOFs (MOF-5 and MOF-177) [7] and only a few times for other porous materials such as active carbons [8–10] and zeolites [7,11–15]. Dissociative N$_2$O chemisorption is a widely used method for the characterization of metal-containing (especially copper-containing) catalysts [16,17]. N$_2$O is among the most powerful greenhouse [18] and ozone-depleting [19] gases and thus its removal from industrial waste gases is an important task [20]. Catalytic decomposition is a normally used approach for N$_2$O

removal [21]. Adsorptive removal of N$_2$O by using metal-exchanged zeolites has been proposed for the cases where catalytic decomposition is not feasible economically due to very low N$_2$O concentration [22,23]. In this manuscript we describe N$_2$O adsorption on MFU-4l [24] and its Li- and Cu^I-derivatives. MFU-4l, constructed from deprotonated bis(1H-1,2,3-triazolo-[4,5-b],[4′,5′-i])dibenzo-[1,4]-dioxin BTDD^{2-} ligands and {Zn$_5$Cl$_4$}$^{6+}$ building units, is a large-pore member of the MFU-4 structure family of cubic frameworks featuring exceptionally high thermal and solvolytic stability [25]. MFU-4 was studied for specific gas separation processes, i.e. separation of isotopologues H$_2$ and D$_2$ by quantum sieving [26] and kinetic CO$_2$/N$_2$ separation [27]. MFU-4l was suggested for technically demanding separation of Kr and Xe [28,29]. The SBUs (secondary building units) of this framework contain Kuratowski-type coordination units [30–32] that include one octahedrally coordinated (central) metal ion and four tetrahedrally coordinated (peripheral) metal ions, the latter structurally related to well-known scorpionate complexes [33]. Postsynthetic metal and ligand exchange allows to prepare a large variety of MFU-4l frameworks containing Mn^{II}, Fe^{II}, Co^{II}, Ni^{II}, Cu^{II} and Cu^I ions in peripheral positions [34–36]. Cu^I-MFU-4l was shown to chemisorb reversibly several simple gas molecules (e.g. H$_2$, N$_2$ and O$_2$) [35]. Besides

* Corresponding author.
  E-mail address: dirk.volkmer@physik.uni-augsburg.de (D. Volkmer).

technically relevant applications, studying the adsorption of small gas molecules in MOFs possessing well defined single-site active centers (in contrast to structurally fluctuating species in solutions, zeolites or non-porous solids) might help to understand the role of active sites and to design an optimized framework for gas capture, purification or separation. Detailed studies on metal-exchanged zeolites have shown that the metal ion plays an important role for N_2O sorption properties. Thus, Ba-ZSM-5 was found to be the most efficient material for N_2O adsorption [23]. The enhanced properties of Ba-ZSM-5 in the N_2O adsorption are not related to a specific chemisorption but rather to a strong electrostatic field generated by naked Ba^{2+} ions within the zeolite cavities [23]. A weak binding of the N_2O molecule to Cu^I sites in Cu^I-ZSM-5 has been observed with IR spectroscopy at 110–120 K [37]. Herein, we study the influence of Lewis-acidic metal sites in MFU-4l on N_2O adsorption properties. Since N_2O, possessing only weak dipole moment (0.161 D), is isoelectronic with CO_2 and has very similar physical and physisorption properties [22], comparing the interaction strength for these two molecules will help to find an optimized framework for selective N_2O adsorption.

2. Experimental

All starting materials were of reagent grade and used as received from the commercial supplier. Fourier transform infrared (FTIR) spectra were recorded with an ATR unit in the range 4000–400 cm^{-1} on a Bruker Equinox 55 FT-IR spectrometer. Thermogravimetric analysis (TGA) was performed with a TA Instruments Q500 analyzer in the temperature range of 25–800 °C in flowing nitrogen gas at the heating rate of 5 K min^{-1}. ICP-OES analyses were performed on a Varian VISTA MPX simultaneous spectrometer with a CCD detector. Elemental analyses were measured with a Vario EL III instrument from Elementar Analysensysteme GmbH. Gas sorption isotherms were measured with a BELSORP-max instrument combined with a BELCryo system. Adsorbed amounts are given in cm^3 g^{-1} [STP], where STP = 101.3 kPa and 273.15 K. Prior to measurements, the samples of MFU-4l and Li-MFU-4l were heated at 200 °C for 20 h in high vacuum to remove the occluded solvent molecules. Cu^I-MFU-4l was prepared *in situ* by heating Cu^{II}-MFU-4l−formate under vacuum (10^{-3} mbar) up to 180 °C (with a heating rate of 4 K min^{-1}) and keeping the sample at this temperature for 1 h (as described previously [35]). X-ray powder diffraction measurements of N_2O adsorption at different temperatures and pressures in Cu^I-MFU-4l were performed at the diffractometer I12 at Diamond (UK). All DFT calculations have been performed with the all-electron full-potential code FHI-aims [38,39]. Electronic exchange and correlation was treated on the level of the generalized gradient approximation (GGA) PBE functional [40] for the geometry optimizations and on the level of the hybrid B3LYP functional [41,42] for consecutive single point calculations on these optimized geometries. Dispersive interactions lacking at these levels of theory were considered through the dispersion-correction scheme due to Tkatchenko and Scheffler [43]. Geometry optimization was performed using tight, tier1 basis sets until residual forces fell below 10^{-4} eV/Å. Hybrid B3LYP + TS energetics, corrected for the zero point energy, are the finally presented numbers in the paper. MFU-4l systems are represented by a Scorpionate-type unit with Zn substituting the B−H unit. For N_2O adsorption, both coordination modes, *via* the N- or O-atom, were considered. The final binding geometry discussed here represents the energetically most favorable state.

2.1. Preparation of Li-MFU-4l

LiCl (1.38 g, 32.5 mmol) was dissolved in N,N-dimethylformamide (130 mL) and MFU-4l (0.8 g, 0.634 mmol)

was added to the solution. The reaction mixture was heated for 20 h at 60 °C in a sealed tube. The precipitate was filtered off, washed with DMF, methanol and dichloromethane and dried at 150 °C under vacuum. The yield is close to quantitative. The number of Li$^+$ ions in the formula unit was calculated from the Li/Zn ratio determined by ICP-OES analysis. The slightly yellow product is hygroscopic and may contain variable amount of adsorbed water. Number of Li$^+$ ions in the formula unit: 1.91. Anal. calcd. for $C_{36}H_{12}Cl_2N_{18}O_6Li_2Zn_3$ · 2H$_2$O: C, 38.97; H, 1.45; N, 22.72. Found: C, 39.17; H, 2.11; N, 22.73%. IR (ATR, cm^{-1}): 3079 (w), 1615 (w), 1575 (w), 1461 (s), 1348 (s), 1172 (s), 916 (m), 850 (m), 809 (w), 533 (m), 425 (w). BET surface area (Ar, 87.3 K): 3356 m^2 g^{-1}.

3. Results and discussion

Li-MFU-4l was prepared *via* postsynthetic metal exchange from MFU-4l and LiCl in DMF at 60 °C (Fig. 1). Similarly to a previously described metal exchange with MnCl$_2$, FeCl$_2$, NiCl$_2$ and CuCl$_2$ [35,36], approx. 2 of 4 Zn^{2+} ions in the SBU are substituted at these conditions leading to a framework with the composition [Li$_2$Zn$_3$Cl$_2$(BTDD)$_3$]. Performing the reaction at 140 °C, as described previously for CoCl$_2$ [34], leads to a complete dissolution of MFU-4l. According to the TGA data, which show a weight loss of 3.0% below 100 °C, and furthermore confirmed by elemental analysis, the framework obtained upon drying in vacuum and subsequent exposure to air has a net composition formulated as [Li$_2$Zn$_3$Cl$_2$(BTDD)$_3$] · 2H$_2$O, which corresponds to one bound water molecule per lithium ion. This observation shows immediately that Li$^+$ ions in the SBU of MFU-4l represent centers of much stronger Lewis-acidy as Zn^{II}−Cl units which do not bind water molecules at the same conditions. The isosteric heats of CO_2 and N_2O adsorption in MFU-4l determined from the adsorption isotherms (as described in Supplementary Information) are very similar (16.4 and 17.9 kJ mol^{-1} at 0.35 mmol g^{-1} loading, respectively, see Table 1) and decrease only slightly with increasing loading (Figs. 2 and 3). These values stay in agreement with the DFT-calculated binding energies (Table 1) and correspond to a physisorbed state. Although the Lewis acidity of Zn^{II} is well-documented in the literature [44], Zn^{II}−Cl units within the MFU-4l framework do not coordinate CO_2
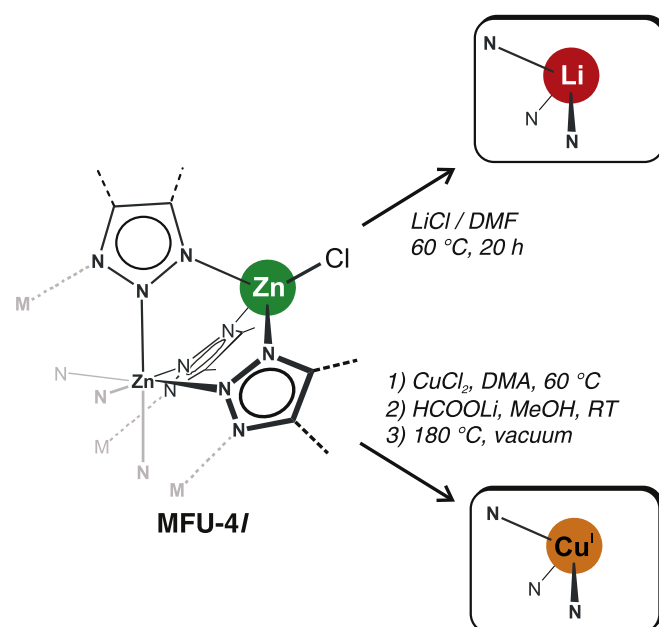

Fig. 1. Preparation of Cu^I- and Li-derivatives of MFU-4l *via* postsynthetic modification.

Table 1
Experimental and DFT-calculated binding energies for CO_2 and N_2O in MFU-4l derivatives.

Compound	Peripheral unit in the SBU	CO_2 binding energy/kJ mol^{-1}		N_2O binding energy/kJ mol^{-1}	
		Experimental[a]	DFT-calculated	Experimental[a]	DFT-calculated
MFU-4l	Zn^{II}–Cl	16.4 ± 0.1	17	17.9 ± 0.3	18
Li-MFU-4l	Li^{I}	22.7 ± 0.9	25	23.6 ± 0.2	25
Cu^{I}-MFU-4l	Cu^{I}	15.3 ± 0.5	18	30.8 ± 1.4	33

[a] Isosteric heat of adsorption at 0.35 mmol g^{-1} loading. Errors are the standard deviations calculated for the linear regression.

or N_2O molecules since this would require an energetically unfavorable distortion of the tetrahedral coordination of the Zn^{II} centers. Li$^+$ ions in the trigonal-pyramidal coordination within the SBU of MFU-4l, in contrast, possess at least one free coordination site which can be filled without any energetic barrier leading to the tetrahedral coordination. A tetrahedral configuration, common for non-transition metal ions, has very often been observed for Li$^+$ [45]. In accordance with this, Li-MFU-4l shows considerably higher isosteric heats of CO_2 and N_2O adsorption (22.7 and 23.6 kJ mol^{-1} at 0.35 mmol g^{-1} loading, respectively, see Table 1) which decrease slowly with increasing loading (Figs. 2 and 3). The values are very similar for both gases as also predicted by our DFT calculations (Table 1) and correspond to a weak interaction of the adsorbed gas
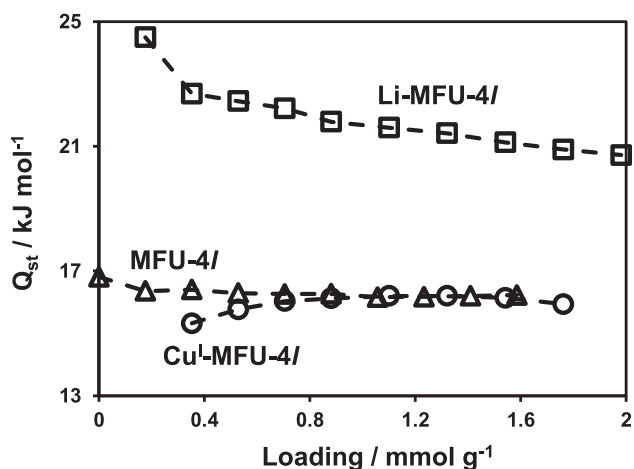

Fig. 2. Dependence of isosteric heats of CO_2 adsorption on loading for MFU-4l (triangles), Cu^{I}-MFU-4l (circles) and Li-MFU-4l (squares).
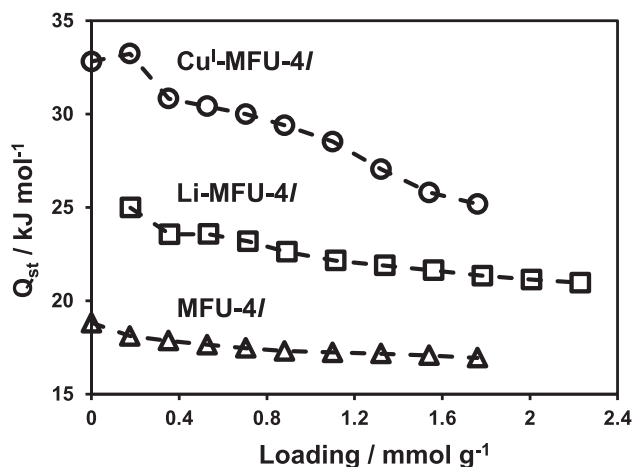

Fig. 3. Dependence of isosteric heats of N_2O adsorption on loading for MFU-4l, Cu^{I}-MFU-4l and Li-MFU-4l.

molecules with the Li$^+$ ions. The weak binding is also confirmed by quite long atomic distances (2.25 Å Li–O distance for CO_2 and 2.35 Å Li–N distance for N_2O) as can be seen from the binding geometries obtained from the DFT calculations (Fig. 4). These results can be well explained within the HSAB (hard and soft (Lewis) acids and bases) concept [46]. Due to this concept, Li$^+$ ions are hard Lewis acids with high charge density (chemical hardness $\eta = 35.12$ eV), whereas CO_2 and N_2O possess quite similar moderate chemical hardness as Lewis bases (8.8 and 7.6 eV, respectively) [47]. This results in a similar moderate binding of CO_2 and N_2O to Li$^+$ ions. The situation is completely different in the case of Cu^I. Thus, Cu^{I}-MFU-4l shows only physisorption of CO_2 (isosteric heat of adsorption 15.3 kJ mol^{-1} at 0.35 mmol g^{-1} loading, see Table 1). DFT calculations predict low interaction energy (Table 1) and large Cu^{I}–CO_2 distance as well (Fig. 5a). N_2O, in contrast, shows quite strong binding to Cu^I centers (isosteric heat of adsorption in Cu^{I}-MFU-4l is 30.8 kJ mol^{-1} at 0.35 mmol g^{-1} loading, see Table 1). The high binding energy for N_2O on Cu^I centers is also confirmed by DFT (Table 1). The calculated binding geometry reveals an almost linear orientation of the N_2O molecule (with respect to the Cu–N bond) and a Cu–N distance of 1.94 Å (Fig. 5b). Both speak for a chemical binding between Cu^I and N_2O. In terms of the HSAB concept, Cu^I is a soft Lewis acid with low charge density (chemical hardness $\eta = 6.28$ eV [47]) and thus it is not surprising that CO_2 doesn't bind to Cu^I. However, a relatively strong binding of N_2O to Cu^I centers cannot be explained easily within the HSAB concept unless N_2O is a slightly softer Lewis base as compared to CO_2. This fact underscores the specific character of the Cu^I–N_2O interaction. Looking at the results of the Hirshfeld charge analysis for Li–N_2O and Cu^I–N_2O adducts within the Kuratowski unit (Table 2) we can see that Li$^+$ ions change their charge from +0.301 to +0.2096 upon N_2O binding. This behavior corresponds to a typical coordinative binding – Li$^+$ acts as a Lewis acid (electron accepting) whereas N_2O serves as a Lewis base (electron donating). Coordination of N_2O molecule to Cu^I center, in contrast, do not lead to a considerable changes of atomic charges (Cu$^+$ changes its charge from +0.22851 to +0.2149) unless even stronger binding is observed. These results might speak for the partial charge transfer from Cu^I to N_2O compensating the coordinative donation of electron density from N_2O to Cu$^+$. Thus, binding of N_2O to Cu^I might be related to the charge-donating properties of Cu^I as well as electron accepting properties of N_2O
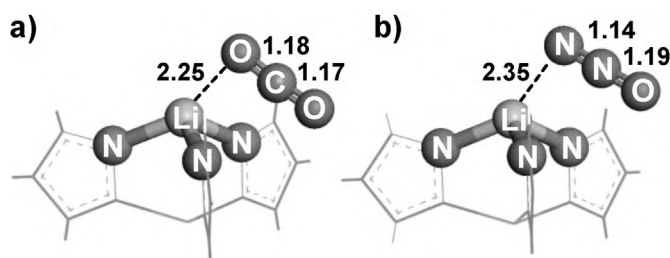

Fig. 4. Binding geometries for CO_2 (a) and N_2O (b) at the Li^I sites within the Kuratowski unit of MFU-4l as obtained from DFT calculations (atomic distances in Å).
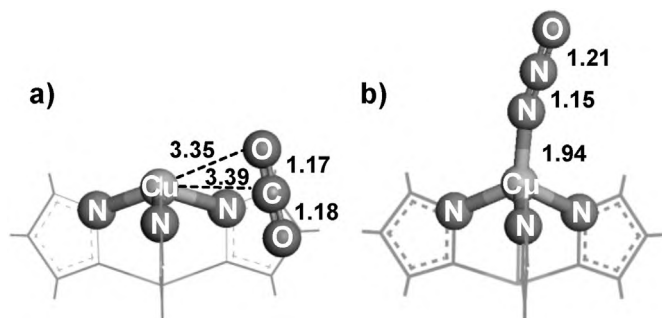
Fig. 5. Binding geometries for CO_2 (a) and N_2O (b) at the Cu^I sites within the Kuratowski unit of MFU-4*l* as obtained from DFT calculations (atomic distances in Å).

Table 2
Hirshfeld charge analysis for Li–N_2O and Cu^I–N_2O adducts within the Kuratowski unit.

Compound/atom[a]	Li-MFU-4*l*		Cu^I-MFU-4*l*	
	Plain[b]	Adduct	Plain[b]	Adduct
M(I)	+0.301	+0.2096	+0.22851	+0.2149
N1	−0.0718	−0.0464	−0.0718	−0.0385
N2	+0.2078	+0.2379	+0.2078	+0.2135
O	−0.1359	−0.0841	−0.1359	−0.1284

[a] M(I) − Li or Cu^I atom of the Kuratowski unit. N1 − terminal N-atom of the N_2O molecule, N2 − the central one.
[b] Plain refers to the Li- or Cu^I−Kuratowski unit and N_2O molecule in the gas phase.

which are reflected in its considerably higher electron affinity as compared to CO_2 [47]. Due to its poor ligand characteristics (low dipole moment and weak σ-donor and π-acceptor properties [48]), N_2O complexes are very rare and have so far only been described for Ru^{II} and V^{III} [49−51].

The preferential binding of N_2O to Cu^I centers is also confirmed by *in situ* synchrotron X-ray powder diffraction measurements. The quality of the data as well as the high temperature of the measurements did not allow the determination of the orientation of the linear N_2O molecule, so that only the approximate position of the center of rotation for the N_2O molecule could be determined. The rotationally (and possibly positionally) disordered N_2O molecule was modeled as a large sphere with a center, coinciding with the center of mass of the molecule. This approximation allows correct determination of positions, but analysis of the N_2O−framework distances is complicated. In total, six adsorption sites were localized. Four of them form a first adsorption layer in the large cavity, one forms a second adsorption layer in the large cavity and one fills the small cavity. The main adsorption positions for the N_2O molecule are the open metal sites, which are located in the small cavity (Fig. 6I, I). The second adsorption site is located in the center of three faces of the $Cu^I N_3$ unit and close to centers of three triazolate rings coordinating metal ions in the SBU (Fig. 6, II, large cavity). The adsorption site III is located near the center of the 1,4-dioxane ring of the organic linker (Fig. 6, III, large cavity). The N_2O molecule is strongly disordered when placed close to this position, and it was refined as occupying a single position, due to the difficulties in the correct description of disorder. The fourth position of the N_2O
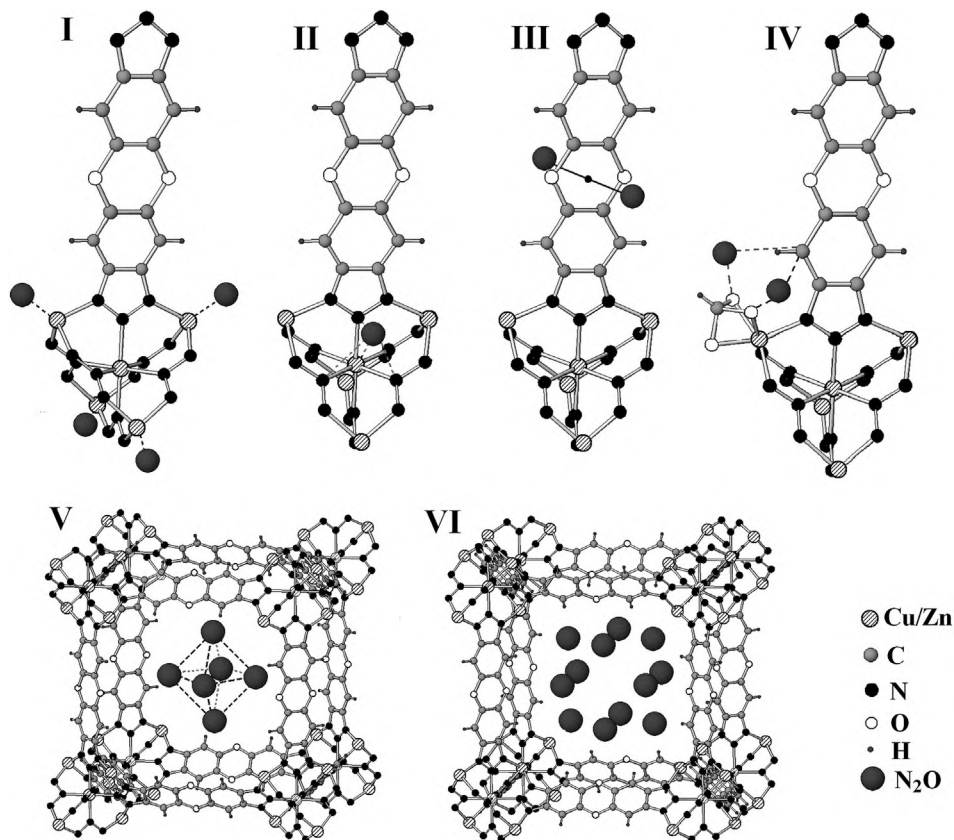

Fig. 6. Six symmetry-independent adsorption sites occupied by N_2O molecule (shown by large spheres) in the pores of Cu^I-MFU-4*l*. These include two sites (I and II) associated with secondary building unit, three sites (III, IV, and V) associated with the organic linker, and one site (VI) forming second adsorption layer within the large pores.

molecule is located near the formate ligand coordinating statistically disordered Zn ions as well as nitrogen and carbon atoms of the triazole- and benzole-rings of the organic linker, respectively (Fig. 6, IV, large cavity). In the fifth position the N_2O molecule is close to the oxygen atoms of the 1,4-dioxane ring of the organic linker (Fig. 6, V, small cavity). A further increase of pressure leads to the formation of the disordered second adsorption layer in the large cavity (Fig. 6, VI). All located positions of N_2O molecule in large and small cavities of Cu^I-MFU-4l are consistent with the previously found positions for noble gas atoms Xe and Ke in Cu^I-MFU-4l [52]. However, the order of their filling is different. No preferential filling of the large cavity in comparison to the small cavity was found for N_2O molecules, and the strongest adsorption site is located near coordinatively unsaturated Cu^I sites.

4. Conclusion

We have studied the interaction strength of N_2O and CO_2 molecules with different Lewis-acidic sites within the MFU-4l metal-organic framework via gas sorption measurements and density-functional theory calculations. Zn^{II}–Cl units appeared to possess only very weak Lewis acidity, such that only physisorption of both gases has been observed. Li^I centers, in contrast, show considerable Lewis acidity and similar binding strength toward N_2O and CO_2 molecules in the gas phase (22.7 and 23.6 kJ mol^{-1} at 0.35 mmol g^{-1} loading, respectively). Cu^I-MFU-4l shows quite strong binding of N_2O, whereas CO_2 doesn't bind to Cu^I centers. Preferential binding of N_2O to Cu^I centers was also confirmed by in $situ$ synchrotron X-ray powder diffraction measurements. Thus, Cu^I-MFU-4l can be considered as a potential candidate for selective N_2O adsorption.

Appendix A. Supplementary data

Supplementary data related to this article can be found at http://dx.doi.org/10.1016/j.micromeso.2015.03.014.

References

[1] H. Furukawa, K.E. Cordova, M. O'Keeffe, O.M. Yaghi, Science 341 (2013) 1230444.
[2] K. Sumida, D.L. Rogow, J.A. Mason, T.M. McDonald, E.D. Bloch, Z.R. Herm, T.-H. Bae, J.R. Long, Chem. Rev. 112 (2012) 724–781.
[3] E. Barea, C. Montoro, J.A.R. Navarro, Chem. Soc. Rev. 43 (2014) 5419–5430.
[4] J.-R. Li, J. Sculley, H.-C. Zhou, Chem. Rev. 112 (2012) 869–932.
[5] M.P. Suh, H.J. Park, T.K. Prasad, D.-W. Lim, Chem. Rev. 112 (2012) 782–835.
[6] Y. Peng, V. Krungleviciute, I. Eryazici, J.T. Hupp, O.K. Farha, T. Yildirim, J. Am. Chem. Soc. 135 (2013) 11887–11894.
[7] D. Saha, Z. Bao, F. Jia, S. Deng, Environ. Sci. Technol. 44 (2010) 1820–1826.
[8] D.O. Shiels, J. Phys. Chem. 33 (1929) 1386–1397.
[9] H. Marsh, T.E. O'Hair, Fuel 45 (1966) 301–309.
[10] Y. Peng, F. Zhang, C. Xu, Q. Xiao, Y. Zhong, W. Zhu, J. Chem. Eng. Data 54 (2009) 3079–3081.
[11] V. Rakić, V. Dondur, S. Gajinov, A. Auroux, Thermochim. Acta 420 (2004) 51–57.
[12] V. Rakić, V. Rac, V. Dondur, A. Auroux, Catal. Today 110 (2005) 272–280.
[13] B.R. Wood, J.A. Reimer, A.T. Bell, J. Catal. 209 (2002) 151–158.
[14] Y. Wang, Z. Lei, B. Chen, Q. Guo, N. Liu, Appl. Surf. Sci. 256 (2010) 4042–4047.
[15] G. Domínguez, R. Hernández-Huesca, G. Aguilar-Armenta, J. Mex. Chem. Soc. 54 (2010) 111–116.
[16] O. Hinrichsen, T. Genger, M. Muhler, Chem. Eng. Technol. 23 (2000) 956–959.
[17] A.V. Zeigarnik, Kinet. Catal. 44 (2003) 233–246.
[18] D.A. Lashof, D.R. Ahuja, Nature 344 (1990) 529–531.
[19] A.R. Ravishankara, J.S. Daniel, R.W. Portmann, Science 326 (2009) 123–125.
[20] V.I. Sobolev, L.V. Pirutko, in: J.C. Taylor (Ed.), Advances in Chemistry Research, vol. 19, Nova Science Publishers, New York, 2013, pp. 1–24.
[21] G. Centi, S. Perathoner, F. Vazzana, CHEMTECH 29 (1999) 48–55.
[22] M.W. Ackley, S.U. Rege, H. Saxena, Micropor. Mesopor. Mat. 61 (2003) 25–42.
[23] G. Centi, P. Generali, L. dall'Olio, S. Perathoner, Ind. Eng. Chem. Res. 39 (2000) 131–137.
[24] D. Denysenko, M. Grzywa, M. Tonigold, B. Streppel, I. Krkljus, M. Hirscher, E. Mugnaioli, U. Kolb, J. Hanss, D. Volkmer, Chem. Eur. J. 17 (2011) 1837–1848.
[25] S. Biswas, M. Grzywa, H.P. Nayek, S. Dehnen, I. Senkovska, S. Kaskel, D. Volkmer, Dalton Trans. (2009) 6487–6495.
[26] J. Teufel, H. Oh, M. Hirscher, M. Wahiduzzaman, L. Zhechkov, A. Kuc, T. Heine, D. Denysenko, D. Volkmer, Adv. Mater. 4 (2013) 635–639.
[27] G. Sastre, J. van den Bergh, F. Kapteijn, D. Denysenko, D. Volkmer, Dalton Trans. 43 (2014) 9612–9619.
[28] A. Soleimani Dorcheh, D. Denysenko, D. Volkmer, W. Donner, M. Hirscher, Micropor. Mesopor. Mat. 162 (2012) 64–68.
[29] A. Soleimani-Dorcheh, R.E. Dinnebier, A. Kuc, O. Magdysyuk, F. Adams, D. Denysenko, T. Heine, D. Volkmer, W. Donner, M. Hirscher, Phys. Chem. Chem. Phys. 14 (2012) 12892–12897.
[30] S. Biswas, M. Tonigold, D. Volkmer, Z. Anorg. Allg. Chem. 634 (2008) 2532–2538.
[31] S. Biswas, M. Tonigold, M. Speldrich, P. Kögerler, M. Weil, D. Volkmer, Inorg. Chem. 49 (2010) 7424–7434.
[32] Y.-Y. Liu, M. Grzywa, M. Tonigold, G. Sastre, T. Schüttrigkeit, N.S. Leeson, D. Volkmer, Dalton Trans. 40 (2011) 5926–5938.
[33] S. Trofimenko, Chem. Rev. 93 (1993) 943–980.
[34] D. Denysenko, T. Werner, M. Grzywa, A. Puls, V. Hagen, G. Eickerling, J. Jelic, K. Reuter, D. Volkmer, Chem. Commun. 48 (2012) 1236–1238.
[35] D. Denysenko, M. Grzywa, J. Jelic, K. Reuter, D. Volkmer, Angew. Chem. 126 (2014) 5942–5946;
Angew. Chem. Int. Ed. 53 (2014) 5832–5836.
[36] D. Denysenko, J. Jelic, K. Reuter, D. Volkmer, Postsynthetic Metal and Ligand Exchange in MFU-4l: a Screening Approach toward Functional Metal-Organic Frameworks Comprising Single-Site Active Centers, Chem. Eur. J. (2015) [accepted].
[37] C. Lamberti, S. Bordiga, M. Salvalaggio, G. Spoto, A. Zecchina, F. Geobaldo, G. Vlaic, M. Bellatreccia, J. Phys. Chem. B 101 (1991) 344–360.
[38] V. Blum, R. Gehrke, F. Hanke, P. Havu, V. Havu, X. Ren, K. Reuter, M. Scheffler, Comp. Phys. Commun. 180 (2009) 2175–2196.
[39] X. Ren, P. Rinke, V. Blum, J. Wieferink, A. Tkatchenko, A. Sanfilippo, K. Reuter, M. Scheffler, New. J. Phys. 14 (2012) 053020.
[40] J.P. Perdew, K. Burke, M. Ernzerhof, Phys. Rev. Lett. 77 (1996) 3865–3868.
[41] A.D. Becke, J. Chem. Phys. 98 (1993) 5648–5652.
[42] P.J. Stephens, J.F. Devlin, C.F. Chabalowski, M.J. Frisch, J. Chem. Phys. 98 (1993) 11623–11627.
[43] A. Tkatchenko, M. Scheffler, Phys. Rev. Lett. 102 (2009) 073005.
[44] Y. Motoyama, H. Nishiyama, in: H. Yamamoto (Ed.), Lewis Acids in Organic Synthesis, vol. 1, WILEY-VCH, Weinheim, 2000, pp. 59–88.
[45] U. Olsher, Chem. Rev. 91 (1991) 137–164.
[46] R.G. Pearson, J. Am. Chem. Soc. 85 (1963) 3533–3539.
[47] R.G. Pearson, Inorg. Chem. 27 (1988) 734–740.
[48] W.B. Tolman, Angew. Chem. 122 (2010) 1034–1041;
Angew. Chem. Int. Ed. 49 (2010) 1018–1024.
[49] J.N. Armor, H. Taube, J. Am. Chem. Soc. 91 (1969) 6874–6876.
[50] C.B. Pamplin, E.S.F. Ma, N. Safari, S.J. Rettig, B.R. James, J. Am. Chem. Soc. 123 (2001) 8596–8597.
[51] N.A. Piro, M.F. Lichterman, W.H. Harman, C.J. Chang, J. Am. Chem. Soc. 133 (2011) 2108–2111.
[52] O.V. Magdysyuk, D. Denysenko, I. Weinrauch, D. Volkmer, M. Hirscher, R.E. Dinnebier, Chem. Commun. 51 (2015) 714–717.